Title
Effect of nitridation on polarity, microstructure, and morphology of AlN films

Journal
Applied Physics Letters, 84(6)

ISSN
0003-6951

Authors
Wu, Y
Hanlon, A
Kaeding, J F
et al.

Publication Date
2004-02-01

Peer reviewed

Dopant activation and ultralow resistance ohmic contacts to Si-ion-implanted GaN using pressurized rapid thermal annealing

Haijiang Yu[a)]
Materials Department and ERATO JST, UCSB Group, University of California, Santa Barbara, California 93106

L. McCarthy and H. Xing
ECE Department, University of California, Santa Barbara, California 93106

H. Waltereit
Materials Department, University of California, Santa Barbara, California 93106

L. Shen and S. Keller
ECE Department, University of California, Santa Barbara, California 93106

S. P. Denbaars, J. S. Speck, and U. K. Mishra
Materials Department and ERATO JST, UCSB Group, University of California, Santa Barbara, California 93106

(Received 22 April 2004; accepted 30 September 2004)

Activation annealing of Si implants in metalorganic-chemical-vapor-deposition-grown GaN has been studied for use in ohmic contacts. Si was implanted in semi-insulating GaN at 100 keV with doses from 5×10^{14} to 1.5×10^{16} cm^{-2}. Rapid thermal annealing at ~1500 °C with 100 bar N_2 overpressure was used for dopant activation, resulting in a minimum sheet resistance of 13.9 Ω/square for a dose of 7×10^{15} cm^{-2}. Secondary-ion-mass-spectroscopy measurements showed a post-activation broadening of the dopant concentration peak by 20 nm (at half the maximum), while x-ray triple-axis $\omega-2\theta$ scans indicated nearly complete implant damage recovery. Transfer-length-method measurements of the resistance of Ti/Al/Ni/Au contacts to activated GaN:Si (5×10^{15} cm^{-2} at 100 keV) indicated contact resistances of 0.07 and 0.02 Ω mm for as-deposited and subsequently annealed contacts, respectively. © *2004 American Institute of Physics*. [DOI: 10.1063/1.1828237]

Ion implantation can facilitate lateral dopant engineering, unannealed ohmic contacts, and etch-free device isolation in AlGaN/GaN high-electron-mobility transistors, thus resulting in devices with higher performance, greater process control, and potentially new device designs. The refractory nature of GaN, however, makes the activation of implants more difficult than in Si and GaAs, with complete implantation damage recovery and dopant activation requiring annealing temperatures above 1500 °C.[1]

Cao *et al.* reported ~90% activation of Si-implanted GaN with a dose of 5×10^{15} cm^{-2} by annealing at 1400 °C in a nitrogen ambient at atmospheric pressure, resulting in an electron mobility of 40 cm^2/V s.[2] Previously, the use of high-temperature activation annealing was complicated by degradation of the exposed GaN surface. In addition, suitably stable capping layers such as AlN were difficult to remove after annealing. For these reasons, post-implantation anneals used in the fabrication of GaN-based electronics have been performed at growth temperatures (~1100 °C) as in the GaN junction field-effect transistor reported by Zolper *et al.*[3] and the ultralow contact resistance achieved by Burm *et al.* on Si-implanted GaN (0.097 Ω mm).[4] Recently, we have observed threading dislocation motion, reaction, and resultant reduction by adopting a rapid annealing technique at 1500 °C with 100 bar N_2 overpressure. A removable AlN capping layer was used to protect the GaN during the anneal, and smooth pit-free surfaces were observed after annealing.[5] The viability of this annealing technique, combined with the ability to completely remove the AlN cap, allows the incorporation of this process into implanted GaN-based devices. In this letter, we report on studies of the activation of Si-implanted GaN using high-temperature high-pressure rapid annealing, leading to the realization of significantly reduced contact and sheet resistances.

Experiments were performed on planar, ~2.5-μm-thick semi-insulating GaN films grown by metalorganic chemical vapor deposition on *c*-plane sapphire. The as-grown lateral resistance of these films was typically in the range of 7×10^9 Ω/square.[6] Si, with doses ranging from 10^{14} to 10^{16} cm^{-2}, was implanted in a series of these samples, with the peak dopant concentration located ~80–100 nm beneath the surface as verified by secondary-ion mass spectroscopy (SIMS) measurements. For doses above 5×10^{15} cm^{-2}, the implantation was carried out at 500 °C to reduce implantation-induced damage. After implantation, samples were capped with 100 nm of reactively sputtered AlN, followed by a dopant activation anneal of ~1500 °C for 1 min with a nitrogen overpressure of ~100 bar. Anneals were performed in a pressure chamber with rf-inductive heating of a graphite susceptor. Surface temperature to rf power calibrations were made using the melting point of solid Si. After the activation anneal, the sputtered AlN cap layer was removed using a KOH-based etchant. The recovery of implantation-induced crystal lattice damage was investigated using x-ray rocking curves and

[a)]Author to whom correspondence should be addressed; electronic mail: hjyu@ece.ucsb.edu

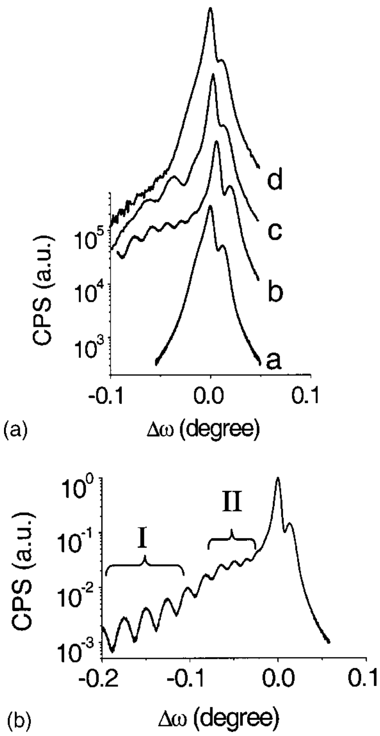

FIG. 1. (a) X-ray triple-axis $\omega-2\theta$ scans of the (0002) reflection from a: as-grown GaN, b: as-implanted GaN with a Si dose of 9×10^{15} cm^{-2}, c: subsequently activated GaN, and d: activated GaN with a Si dose of 5×10^{15} cm^{-2}. (b) X-ray triple-axis $\omega-2\theta$ scan of the (0002) reflection from as-implanted GaN with a Si dose of 9×10^{15} cm^{-2} showing interference fringes with varying spacing caused by swelling of the implanted region. Spacings of ~0.025° (I) indicate a layer thickness of ~200 nm, while the spacing of ~0.014° (II) indicates a layer thickness of ~300 nm.

triple-axis $\omega-2\theta$ scans on the same sample before and after implant and activation. SIMS measurements were performed to measure the Si dopant profile on samples after implantation, and again after activation. The electrical properties of the films were characterized after activation using room-temperature Hall measurements with indium contacts in a van der Pauw geometry on 4×4 mm^2 samples. Ti/Al/Ni/Au (200/1500/375/500 Å) contacts (100×200 μm^2) were then deposited in a transfer-length-method (TLM) pattern on an activated sample with a Si implant dose of 5×10^{15} cm^{-2} at 100 keV. TLM structures were isolated using Cl_2 reactive ion etching and pattern dimensions were confirmed using scanning electron microscopy. Next, contact resistances were measured using a four-wire Kelvin method before and after a contact anneal at 870 °C for 30 s.

X-ray triple-axis $\omega-2\theta$ scans of the (0002) GaN reflection of implanted samples [Fig. 1(a)] showed evidence of lattice expansion of surface layers. Varying degrees of expansion were indicated by a change in the spacing of fringes caused by interference between damaged and underlying GaN layers [Fig. 1(b)]. The spacing of fringes (~0.014°) on the lower 2θ side nearest the undamaged GaN Bragg peak corresponds to a layer thickness of ~300 nm, while the larger fringe spacing (~0.025°) farther from the undamaged peak on the lower 2θ side corresponds to a layer thickness of 200 nm. X-ray scans of annealed samples with ion doses below 9×10^{15} cm^2 did not have these interference fringes, indicating nearly complete recovery of the lattice damage. For higher doses, shoulder peaks observed in scans taken after annealing indicate a degree of unrecovered damage.

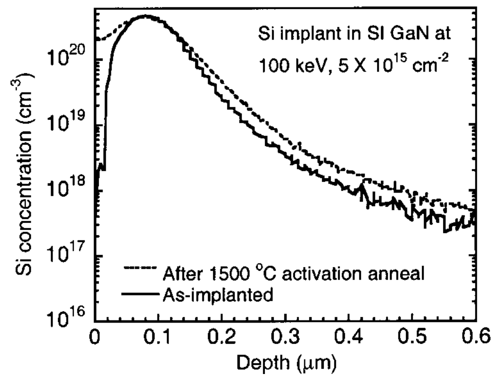

FIG. 2. SIMS profiles of implanted Si (5×10^{15} cm^{-2} at 100 keV) in semi-insulating GaN.

The side peak on the higher 2θ side of the main Bragg peak evident in all scans is characteristic of the semi-insulating buffer structure and is not associated with ion implantation.

SIMS results before and after activation of a sample with an implantation dose of 5×10^{15} cm^{-2} (Fig. 2) showed a peak dopant concentration of $\sim4\times10^{20}$ cm^{-3}, and an as-implanted dopant distribution with a full width at half-maximum (FWHM) of ~90 nm. After implant activation, the FWHM of the Si concentration profile was increased by ~20 nm. A rough estimate (using $D=l^2/t$, where l is the widening of FWHM and t is the heating duration) gives a diffusion constant $D=7\times10^{-14}$ cm^2 s^{-1} at ~1500 °C with a 100 bar N_2 overpressure.

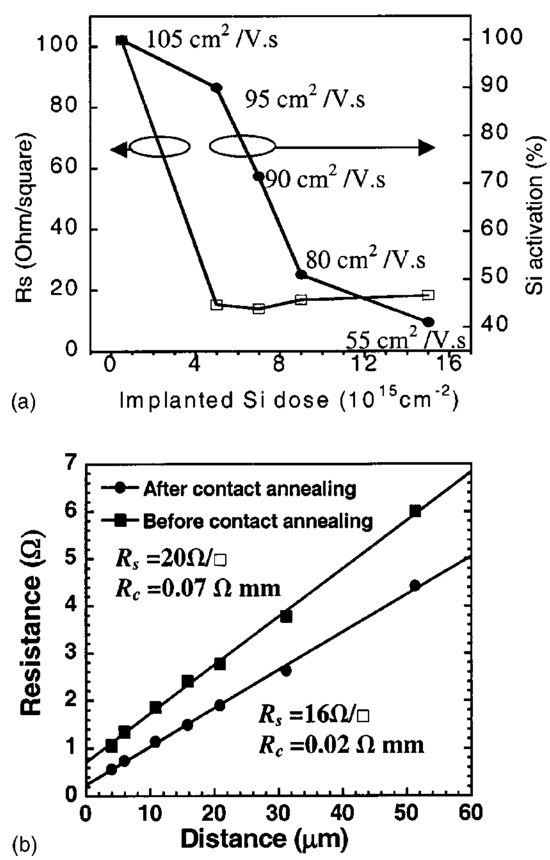

FIG. 3. (a) Hall measurement of sheet resistance as a function of Si dose implanted at 100 keV (with corresponding mobility indicated) and activation efficiency after annealing. Implantation doses above 7×10^{15} cm^{-2} were performed at 500 °C, with lower doses at room temperature. (b) TLM measurement of contact resistance for nonalloyed and alloyed contacts to activated GaN:Si with an implant dose of 5×10^{15} cm^{-2} at 100 keV.

The transport properties of activated samples were measured using Hall and TLM techniques. Figure 3 shows a minimum sheet resistance of 14 Ω/square with a sheet carrier concentration of 5×10^{15} cm^{-2} and Hall electron mobility of 90 cm^2/V s. As the Si implantation dose increased from 5×10^{14} to 1.5×10^{16} cm^{-2}, the activation efficiency decreased from nearly 100% to 41%. For doses above 5×10^{15} cm^{-2}, the sheet resistance decreased and saturated at 15 Ω/square. The lower activation efficiency and carrier mobilities for heavily implanted films may be related to unrecovered damage to the crystal, as indicated by the x-ray results above. TLM measurements (Fig. 3) were performed on a sample with a Si implantation dose of 5×10^{15} cm^{-2}. The current range used was from −25 to 25 mA/mm with resistances taken at zero current. The measured resistance was plotted as a function of the spacing between the contacts before and after the contact annealing step. The sheet resistance determined from this measurement agreed with Hall results, and although still under investigation, the slight reduction in measured sheet resistance after the contact anneal may be related to further damage recovery or implant activation during the contact anneal. The contact resistance was determined from the intercept of the least square linear fit of the TLM measurements, with values of 0.07 and 0.02 Ω mm for nonalloyed and alloyed contacts, respectively. For the as-deposited contacts, we extracted a specific contact resistance of 4.5×10^{-6} Ω cm^2.

The specific contact resistance was not extracted for the annealed contacts because its determination in this case is complicated by the difficulty in determining the transfer length L_T, as

$$L_T = \frac{R_{\mathrm{sh}}}{2R_{\mathrm{sk}}} L_x, \tag{1}$$

where R_{sh} and R_{sk} are the sheet resistance between and under the contact pads respectively, and L_x is the intercept of the least-squares linear fit line with the distance axis in the plot.[7] Because differences between R_{sh} and R_{sk} can lead to orders of magnitude overestimation of the transfer length, using this calculation for annealed contacts may lead to incorrect results. Considering these difficulties, the linear contact resistance is a more reliable figure of merit for annealed ohmic contacts than is the specific contact resistance.

The extremely low contact resistance (0.07 Ω mm) for nonalloyed contacts can be attributed to the heavy *n*-type doping of the implanted GaN, while the reduction of the contact resistance after the contact anneal to 0.02 Ω mm may be the result of contacts spiking through the surface layer of GaN, accessing the concentration peak of implanted Si located ~80 nm beneath the GaN surface. We expect that a lower contact resistance is possible through the further optimization of implantation conditions.

The work of one author (H.Y.) was supported by the JST ERATO program at UCSB, while support for the collaborating authors and special equipment was provided by the AFOSR (G. Witt) and the ONR (H. Dietrich).

[1] S. O. Kucheyev, J. S. Williams, and S. J. Pearton, Mater. Sci. Eng., R. **33**, 51 (2001).
[2] X. A. Cao, S. J. Pearton, R. K. Singh, C. R. Abernathy, J. Han, R. J. Shul, D. J. Rieger, J. C. Zolper, R. G. Wilson, M. Fu, J. A. Sekhar, H. J. Guo, and S. J. Pennycook, MRS Internet J. Nitride Semicond. Res. **4S1**, G6.33 (2000).
[3] J. C. Zolper, R. J. Shul, A. G. Baca, R. G. Wilson, S. J. Pearton, and R. A. Stall, Appl. Phys. Lett. **68**, 2273 (1996).
[4] J. Burm, K. Chu, W. A. Davis, W. J. Schaff, L. F. Eastman, and T. J. Eustis, Appl. Phys. Lett. **70**, 464 (1997).
[5] Haijiang Yu, F. Wu, L. McCarthy, S. Keller, S. P. Denbaars, J. S. Speck, and U. K. Mishra, *ICNS-5 Technical Digest*, Nara, Japan, May 2003, p. 70.
[6] S. Heikman, S. Keller, S. P. DenBaars, and U. K. Mishra, Appl. Phys. Lett. **81**, 439 (2003).
[7] G. K. Reeves and H. B. Harrision, IEEE Electron Device Lett. **EDL-3**, 111 (1982).